THE ASTROPHYSICAL JOURNAL, 484:108–117, 1997 July 20

LEARNING ABOUT ACTIVE GALACTIC NUCLEUS JETS FROM SPECTRAL PROPERTIES OF BLAZARS

MAREK SIKORA,[1,2] GREG MADEJSKI,[2,3] RAFAŁ MODERSKI,[1] AND JURI POUTANEN[4,5]

Received 1996 July 30; accepted 1997 February 14

ABSTRACT

We use multiwavelength spectra of core-dominated flat spectrum radio-loud quasars (FSRQs) to study properties of jets in active galactic nuclei. From a comparison of the predicted bulk Compton radiation with the observed soft X-ray fluxes, we find that these jets must be optically very thin. This eliminates the importance of such processes as Coulomb interactions, pair annihilation, and bremsstrahlung and determines the minimum distance from the black hole where a powerful jet can be fully developed (accelerated, collimated, and mass loaded). In the case of pair dominated jets, this distance is $\gg 100GM_{\rm BH}/c^2$.

Further constraints on the parameters of a jet can be derived from luminosities and positions of spectral peaks of low-energy (IR/optical) and high-energy (γ-ray) radiation components, provided that both are produced by the same population of electrons. Whereas there appears to be a consensus about the synchrotron origin of the low-energy component, there is still debate about the mechanism of production of γ-rays. Most likely, they result from Comptonization of a soft radiation field by the same electrons that produce synchrotron radiation. Such a soft radiation field can be provided by the synchrotron process in a jet, by the accretion disk, and by a fraction of the disk radiation that is reprocessed/rescattered by emission line clouds, dust, and intercloud medium. We show that for FSRQs, the production of the high-energy radiation can be dominated by Comptonization of synchrotron radiation only for jets with moderate bulk Lorentz factors Γ_j ($\lesssim 3$) or if external radiation fields are much weaker than those observed in typical quasars. Furthermore, in synchrotron self-Compton (SSC) models, the relativistic plasma producing nonthermal radiation is constrained to be very weakly magnetized ($B' < 0.01$ gauss) and located at very large distances ($r \sim 10^{19}$ cm). These can impose problems with jet confinement and with short observed timescale of variability. In the external radiation Compton (ERC) models, the magnetic fields are predicted to be much stronger ($B' \sim 100$ gauss), and nonthermal radiation can be produced very closely to the black hole ($r \sim 10^{16}$ cm), which alleviates the problems with plasma confinement and short timescale variability. However, because of the close proximity to the black hole, the constraints imposed by the bulk Compton radiation imply that the plasma must be free of e^+e^- pairs.

Finally, we discuss the difficulties that existing models have in explaining the sharp spectral breaks at MeV energies and postulate a "hot electron" version of the ERC scenario for the production of MeV peaks. We show that appropriate electron "temperatures" ($kT \sim 100$ MeV) to produce the luminosity peak at MeV energies by Comptonization of external UV radiation are achievable at subparsec distances only for proton-electron plasmas.

Subject headings: galaxies: jets — gamma rays: theory — radiation mechanisms: nonthermal

1. INTRODUCTION

Studies of extended double radio structures in radio-loud quasars show that they must be powered at a rate of 10^{46}–10^{47} ergs s^{-1} (Rawlings & Saunders 1991). Such a large power can be provided only by the release of energy in the innermost parts of an accretion disk (Blandford & Payne 1982) or by fast-rotating black holes (Blandford & Znajek 1977). From radio observations on a parsec and larger scales we know that this energy is transmitted outward by highly collimated relativistic jets. Perhaps the most detailed study of these jets is afforded via the interpretation of observations of objects where the jets are believed to point closely to our line of sight. These objects are blazars, a class of active galactic nuclei (AGNs) that encompasses flat spectrum radio quasars (FSRQs) as well as BL Lac objects (for a review, see, e.g., Sikora 1994). Such jets, if starting near the black hole, are expected to undergo strong Compton interactions with the surrounding dense radiation fields. In particular, cold electrons streaming in a jet together with protons at bulk Lorentz factors $\Gamma_j \sim 10$ (which is a typical value inferred from VLBI measurements; see, e.g., Vermeulen & Cohen 1994) are expected to produce strong-beamed soft X-ray flux due to Comptonization of external UV radiation (Begelman & Sikora 1987). As a result, spectra of blazars should show prominent soft X-ray bumps/excesses, which are *not* observed. This suggests that at least in quasars—where UV radiation fields are very dense—the jets must be accelerated, collimated, and/or mass loaded, (Levinson 1996a) over a much larger distance range than the size of the central engine.

Further probing of the subparsec jets can be accomplished by the use of nonthermal spectra of FSRQs. These spectra are dominated by two broad components: one at low energies, peaking in the IR band, and another at high

[1] Nicolaus Copernicus Astronomical Center, Bartycka 18, 00-716 Warsaw, Poland; sikora@camk.edu.pl, moderski@camk.edu.pl.
[2] Laboratory for High Energy Astrophysics, NASA/GSFC, Greenbelt, MD 20771; madejski@lheavx.gsfc.nasa.gov.
[3] Department of Astronomy, University of Maryland, College Park, MD 20742.
[4] Stockholm Observatory, S-133 36 Saltsjöbaden, Sweden; juri@astro.su.se.
[5] Uppsala Observatory, S-751 20, Uppsala, Sweden.

energies, peaking in the γ-ray band, often at MeV energies (von Montigny et al. 1995; see Fig. 1). Highly polarized and variable infrared and optical radiation is successfully interpreted in terms of Doppler-boosted synchrotron radiation (Blandford & Rees 1978; Blandford & Königl 1979), while the most plausible mechanism of the γ-ray production seems to be Compton upscattering of lower energy photons; both processes are most likely due to electrons with random relativistic energies ranging up to 10^3–$10^5 m_e c^2$. Since the timescales of radiative energy losses of such electrons are very short to both synchrotron and Compton processes, the electrons must be accelerated in situ, i.e., in the regions where they produce radiation. These seed photons can be provided by the synchrotron radiation in a jet (Rees 1967; Königl 1981; Marscher & Gear 1985; Ghisellini & Maraschi 1989), by external sources (Dermer, Schlickeiser, & Mastichiadis 1992; Dermer & Schlickeiser 1993; Sikora, Begelman, & Rees 1994, hereafter SBR; Blandford & Levinson 1995; Levinson & Blandford 1995), and/or by jet synchrotron radiation reprocessed/rescattered by external matter/clouds located very closely to the jet (Ghisellini & Madau 1996).

The relative contribution of these soft radiation fields as "seeds" for Comptonization depends on their energy density as measured in the comoving frame of the jet. As it was demonstrated by SBR and Sikora et al. (1996), in the case of quasars, the largest contribution appears to be from the diffuse external radiation fields produced by reprocessing/rescattering of the accretion disk radiation by emission line clouds, dust, and intercloud medium. From the measured luminosities and energies of the spectral peaks of the low-energy (synchrotron) and the high-energy (Compton) components, it is possible to estimate Poynting fluxes and magnetic field intensities and then distances at which most of the nonthermal radiation is produced, as well as the maximum content of e^+e^- pairs in the jets. We show that these results are dramatically different for synchrotron self-Compton models (SSC) and external radiation Compton (ERC) models.

Additional constraints on the relative importance of various radiation models can be obtained from the X-ray spectra and from the change of the spectral slope in the vicinity of the MeV peaks. The average energy index of X-ray spectra in FSRQs is $\alpha \simeq 0.7$ (Worrall & Wilkes 1990; Kii et al. 1992; McNaron-Brown et al. 1995). As was pointed out by Ghisellini & Madau (1996), such hard spectra cannot be reproduced by ERC models with pair cascades (see Svensson 1987 for the discussion of the dependence of the spectral slope on the number of electron generations in the pair cascade process). With regard to the MeV spectral break, in most cases, the slope change is $\Delta\alpha \leq 0.5$, which can be explained by homogeneous version of ERC model in terms of incomplete cooling of relativistic electrons below certain energy. However, some FSRQs show $\Delta\alpha \geq 1$ (McNaron-Brown et al. 1995; Blom et al. 1995; Bloemen et al. 1995). Such breaks accompanied by hard X-ray spectra cannot be reproduced by any existing homogeneous model, unless one postulates an ad hoc break in the electron injection function. γ-ray spectra that are sharply peaked in the MeV range—accompanied by hard X-ray spectra—*can* in fact be explained by pair-free inhomogeneous models, but in such models, the relativistic electron energy distribution must be fine-tuned to avoid any intensive pair production at *any* distance, and the product of the maximum electron energy in the region where MeV peak is produced times Γ_j must always be $\sim 10^3$ MeV in order to upscatter external UV photons up to MeV energies. Alternative possibility, which we postulate in this paper, is the "hot electron" version of the ERC model, where the MeV peak is produced by electrons that undergo very efficient heating process such that at distances of 10^{17}–10^{18} cm they reach a "temperature" of ~ 100 MeV.

Our paper is organized as follows. In § 2, we compare the soft X-ray fluxes predicted by the bulk Compton process with the observations and derive constraints on the optical thickness and distance where the AGN jet is formed. In § 3, we use the luminosities and locations of the two spectral components in FSRQs to derive constraints on the SSC and ERC models. In § 4, we review the difficulties that all existing models have in reproducing the large spectral breaks at MeV peaks, and we propose a "hot electron" version of the ERC model to explain the extreme cases of the MeV radiation–dominated FSRQs. Our results are summarized in § 5.

2. SOFT X-RAYS VERSUS BULK COMPTON RADIATION PREDICTIONS

We assume that the plasma flows in a steady jet, which propagates at a constant bulk Lorentz factor Γ_j and has conical geometry with an opening angle $\theta_j \sim 1/\Gamma_j$; we compare this configuration of a jet to that consisting of individual "blobs" in Appendix B. In addition to highly relativistic electrons and positrons (hereafter together called electrons), the jet is very likely to contain electrons that are cold (nonrelativistic in the jet frame). Streaming through external radiation fields, such cold electrons produce bulk Compton luminosity (defined under an assumption of isotropy, i.e., as $L = 4\pi d_L^2 F_{\rm obs}$, where d_L is the luminosity distance to the source and $F_{\rm obs}$ is the measured flux)

$$L_{\rm BC,em} = \int_{r_{\rm min}} \left| \frac{dE_e}{dt} \right| n_e \, dV \, , \tag{1}$$

where $|dE_e/dt|$ is the Compton energy losses rate of electrons, n_e is the number density of nonrelativistic electrons as measured in the black hole frame, $dV \simeq \pi a^2 \, dr$ is the volume element, $a \sim r\theta_j \sim r/\Gamma_j$ is the cross-sectional radius of a jet, r is the distance from the apex of the cone, and $r_{\rm min}$ is the distance at which the jet is assumed to be not fully developed yet, i.e., not sufficiently accelerated, collimated, or mass loaded to contribute significantly to the bulk Compton radiation.

Assuming that $\Gamma_j > \Gamma_{\rm eq}$, where $\Gamma_{\rm eq}$ is the Lorentz factor of the frame in which an external radiation field has zero net flux at the jet axis (Sikora et al. 1996), the electron energy losses can be approximated by the formula

$$\left| \frac{dE_e}{dt} \right| \simeq c\sigma_{\rm T} \Gamma_j^2 u_D \, , \tag{2}$$

where

$$u_D = \frac{\xi L_{\rm UV}}{4\pi r^2 c} \tag{3}$$

is the energy density of an external diffuse radiation field, $L_{\rm UV}$ is the luminosity of the central source (which in quasars is dominated by UV radiation of an accretion disk), and ξ is the fraction of UV radiation, which at a given distance r

contributes to the diffuse (isotropized by reprocessing and/or rescattering) radiation field. For quasars, the fraction ξ is expected to be ~ 0.01–0.1. In the vicinity of the black hole, ξ is determined by Thomson optical depth of disk coronae/winds, while at larger distances, it is determined by the fraction of the central radiation converted to broad emission lines by optically thick clouds, and to IR radiation by dust. As was shown by Sikora et al. (1996), with all these quasar radiation components, $\Gamma_{\rm eq} < 4$ up to distances $r \sim 10^4 r_g$, which justifies the use of the approximate formula (2), provided $\Gamma_j > 5$ ($r_g = GM_{\rm BH}/c^2$ is the gravitational radius).

Assuming that the flux of cold electrons is conserved along the jet (no pair production or annihilation at $r > r_{\rm min}$), we have $n_e \propto 1/r^2$. Using this in equation (1) and inserting equations (2) and (3), we obtain[6]

$$L_{\rm BC,em} \simeq \frac{n_e(r_{\rm min}) r_{\rm min}\, \sigma_T\, \xi L_{\rm UV}}{4} . \tag{4}$$

The bulk Compton radiation is beamed along the jet axis; the observer, located at $\theta_{\rm obs} \sim 1/\Gamma_j$ will see $L_{\rm BC} \sim 2\Gamma_j^2 L_{\rm BC,em}$ (see Appendix A). This luminosity should be peaked at energy

$$h\nu_{\rm BC} \simeq \Gamma_j^2\, h\nu_{\rm uv} \sim \left(\frac{\Gamma_j}{10}\right)^2 \ {\rm keV} , \tag{5}$$

i.e., in soft X-rays, precisely where the γ-ray dominated blazars show strong deficiency of radiation (see Fig. 1).

For a given distance r, the optical thickness to Thomson scattering by cold electrons in the jet is given by $\tau_j \simeq n_e a \sigma_T \simeq n_e r \sigma_T/\Gamma_j$. Using the observational constraint $L_{\rm BC} \leq L_{\rm SX}$, where $L_{\rm SX}$ is the observed luminosity at $\nu \sim \nu_{\rm BC}$, it follows that

$$\tau_j(r_{\rm min}) \lesssim 0.02\, \frac{L_{\rm SX,46}}{(\xi L_{\rm UV})_{45}} \left(\frac{\Gamma_j}{10}\right)^{-3} , \tag{6}$$

where $L_{\rm SX,46} = L_{\rm SX}/10^{46}$ ergs s^{-1} and $(\xi L_{\rm UV})_{45} = \xi L_{\rm UV}/10^{45}$ ergs s^{-1}.

Thus, highly relativistic and collimated jets must be optically very thin, since high optical thickness predicts higher-than-observed soft X-ray flux. This imposes serious constraints on any radiation models that involve such processes as pair annihilation, bremsstrahlung, and Coulomb interactions. This is because in such thin plasmas, the timescales of these processes are much longer than the timescale of plasma propagation in a jet (Coppi & Blandford 1990).

So far, we did not specify the normalization of the electron number density. Such normalization is provided by the formula for kinetic luminosity of a jet, which in case of inertia dominated by cold protons ($n_e/n_p < m_p/m_e$) is

$$L_K \simeq n'_p m_p c^3 \pi a^2 \Gamma_j^2 \sim n'_p m_p c^3 \pi r^2 , \tag{7}$$

where n'_p is the number density of protons in the jet comoving frame. Noting that $n_p = n'_p \Gamma_j$, we have

$$n_e \simeq \frac{n_e}{n_p} \frac{L_K \Gamma_j}{\pi m_p c^3 r^2} . \tag{8}$$

[6] Equation (4) is derived assuming $\partial\xi/\partial r = 0$. However, the result should be of the same order also for $\partial\xi/\partial r \neq 0$, provided the dependence of ξ on r is weaker than the dependence of n_e on r.

Substituting this into the formula for $L_{\rm BC}$ for $r = r_{\rm min}$, we obtain

$$L_{\rm BC} \simeq 2\, \frac{n_e}{n_p} \frac{r_g}{r_{\rm min}} \frac{L_K}{L_{\rm Edd}}\, \xi L_{\rm UV} \Gamma_j^3 , \tag{9}$$

where $L_{\rm Edd} = (4\pi m_p c^3/\sigma_T) r_g$. Then, the condition $L_{\rm BC} \leq L_{\rm SX}$ gives

$$\frac{r_{\rm min}}{r_g} \geq 200\, \frac{n_e}{n_p} \frac{L_K}{L_{\rm Edd}} \frac{(\xi L_{\rm UV})_{45}}{L_{\rm SX,46}} \left(\frac{\Gamma_j}{10}\right)^3 , \tag{10}$$

which implies that for powerful ($L_K \sim L_{\rm Edd}$) and pair-dominated ($n_e \gg n_p$) jets, overproduction of soft X-rays can be avoided only if $r_{\rm min} \gg 200 r_g$. (Note that for $n_e/n_p > m_p/m_e$, the inertia of jet is dominated by cold electrons, and the term $n'_p m_p$ in eq. [7] must be replaced by $n'_e m_e$, and then the term n_e/n_p in eqs. [8], [9], and [10] must be replaced by m_p/m_e.)

3. CONSTRAINTS DERIVED FROM THE BROADBAND SPECTRA

3.1. *SSC Model versus ERC Model*

The broadband spectra of blazars consist of two prominent, broad components, one at low energy, peaking in the IR through optical bands, and another at high energy, peaking in γ-rays (see Fig. 1). While the low-energy component is most likely produced by synchrotron radiation (Blandford & Rees 1978; Blandford & Königl 1979), the high-energy component is presumably produced by an inverse Compton process, and thus the emission in both components requires relativistic electrons. The seed photons for the Compton process can be provided either by synchrotron radiation in a jet or by external sources (see § 1 and the review by Sikora 1994). The criterion determining which radiation field dominates in the Compton energy losses of relativistic electrons can be derived from the comparison of energy densities of these radiation fields in the comoving frame of the jet. Noting that energy density of the synchrotron radiation is

$$u'_S \simeq \frac{L_S}{4\pi a^2 c \Gamma_j^4} \sim \frac{L_S}{4\pi r^2 c \Gamma_j^2} , \tag{11}$$

where L_S is the luminosity of synchrotron radiation, and that the energy density of radiation fields provided by external sources is $u'_D \sim \Gamma_j^2 u_D$, where u_D is given by equation (3), we find that SSC mechanism can dominate over ERC only if

$$\Gamma_j < \left(\frac{L_S}{\xi L_{\rm UV}}\right)^{1/4} \simeq 3 \left[\frac{L_{\rm S,47}}{(\xi L_{\rm UV})_{45}}\right]^{1/4} , \tag{12}$$

or

$$\xi < 10^{-3}\, \frac{L_{\rm S,47}}{L_{\rm UV,46}} \left(\frac{\Gamma_j}{10}\right)^{-4} . \tag{13}$$

Since in quasars the reprocessed/rescattered continuum can easily provide $\xi L_{\rm UV} \sim 10^{44}$–$10^{45}$ ergs s^{-1}, while statistical analyses (Padovani & Urry 1992; Maraschi & Rovetti 1994) and VLBI observations (Vermeulen & Cohen 1994) give $\Gamma_j > 5$, the production of γ-rays in jets of FSRQs is most likely dominated by the ERC mechanism.

It should be emphasized here that equation (11), and therefore conditions (12) and (13), apply for both steady sources and moving patterns (" blobs ") (see Appendix B).

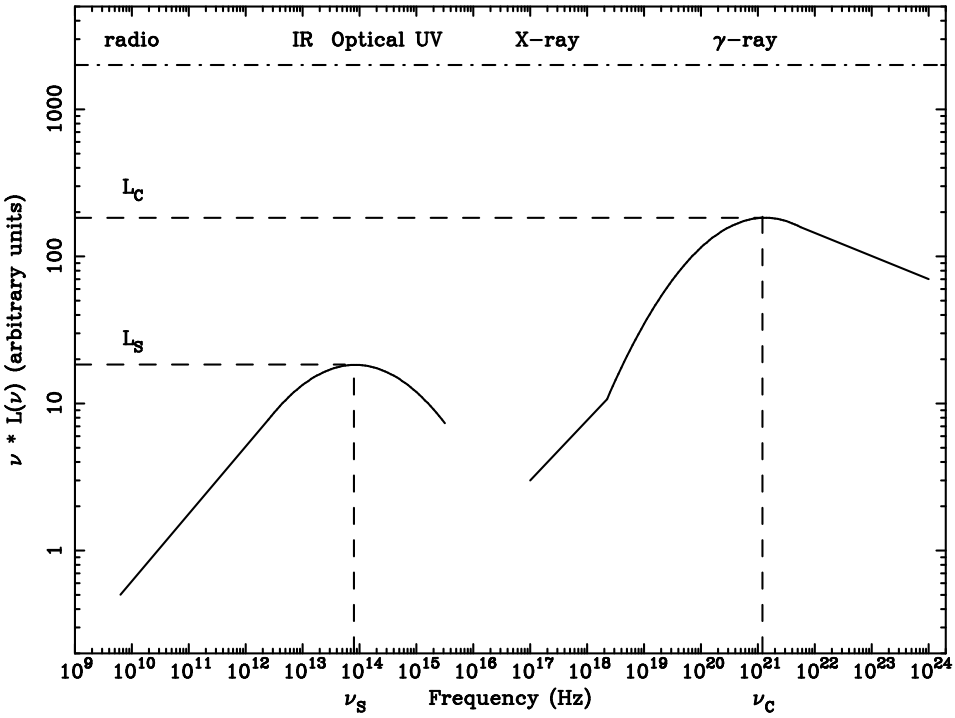

FIG. 1.—Schematic representation of a spectrum of an MeV blazar

3.2. *Other Constraints on SSC models*

3.2.1. *Poynting Flux*

If both high-energy and low-energy spectral components are produced by the same population of relativistic electrons, and the production of high-energy radiation is dominated by the SSC process, then

$$\frac{L_C}{L_S} \sim \frac{L'_C}{L'_S} \sim \frac{u'_S}{u'_B}, \tag{14}$$

where $u'_B = (B')^2/8\pi$ is the energy density of magnetic field. Equations (11) and (14) thus give

$$u'_B \simeq \frac{1}{4\pi r^2 c\Gamma_j^2}\frac{L_S^2}{L_C}, \tag{15}$$

which, in the case of steady flow, determines the Poynting flux

$$L_B \simeq cu'_B \pi a^2 \Gamma_j^2 \simeq cu'_B \pi r^2 \simeq \frac{1}{4\Gamma_j^2}\frac{L_S^2}{L_C}$$
$$\simeq 2.5 \times 10^{43}\frac{L_{S,47}^2}{L_{C,48}}\left(\frac{\Gamma_j}{10}\right)^{-2} \text{ ergs s}^{-1}. \tag{16}$$

Thus, luminosities of high- and low-energy components in the γ-ray–radiation–dominated FSRQs can be explained in terms of the SSC model only for very weakly magnetized jets, with L_B about 3 orders of magnitude lower than the power that must be delivered to the radio lobes in radio-loud quasars (Rawlings & Saunders 1991).

3.2.2. *Electron Energies and Magnetic Fields*

Using δ-approximations for photon energies at luminosity peaks, $h\nu_S$ and $h\nu_C$ (see Fig. 1), one can derive the energies of electrons that produce these peaks, γ'_b, and magnetic fields in the region where the peaks are produced (see, e.g., Ghisellini, Maraschi, & Dondi 1996). For photons produced by synchrotron radiation we have

$$h\nu'_S \simeq (\gamma'_b)^2 (B'/B_{\rm cr}) m_e c^2, \tag{17}$$

and for photons resulting from Compton upscattering of synchrotron photons we have

$$\nu'_C \simeq (\gamma'_b)^2 \nu_{sS'}, \tag{18}$$

where $\nu'_S \simeq \nu_S/\Gamma_j$, $\nu'_C \simeq \nu_C/\Gamma_j$, and $B_{\rm cr} \equiv m_e^2 c^3/\hbar e \simeq 4.4 \times 10^{13}$ gauss. These equations give

$$\gamma'_b \simeq \left(\frac{\nu'_C}{\nu'_S}\right)^{1/2} \simeq 10^4 \left(\frac{\nu_{C,21}}{\nu_{S,13}}\right)^{1/2}, \tag{19}$$

and

$$B' \simeq \frac{h\nu'_S/m_e c^2}{(\gamma'_b)^2} B_{\rm cr} \simeq 4 \times 10^{-3}\frac{\nu_{S,13}^2}{\nu_{C,21}}\left(\frac{\Gamma_j}{10}\right)^{-1} \text{ gauss}, \tag{20}$$

where $\nu_{S,13} = \nu_S/10^{13}$ Hz and $\nu_{C,21} = \nu_C/10^{21}$ Hz.

3.2.3. *Distance, Pair Content, and Variability Timescales*

Combining equation (20) with equation (15) or equation (16), one can find that the distance at which the synchrotron and Compton luminosity peaks are produced is

$$r_{\rm SSC} \simeq 2 \times 10^{19}\frac{\nu_{C,21}}{\nu_{S,13}^2}\frac{L_{S,47}}{L_{C,48}^{1/2}} \text{ cm}. \tag{21}$$

This is $\sim 10^5 r_g$ for a black hole with mass $\sim 10^9 M_\odot$.

At such distances, the models of even strongly pair-dominated jets are so optically thin that they do not overproduce soft X-rays due to bulk Compton radiation (see § 2). However, provided the jet is fully developed already at $r_{\rm min} \ll r_{\rm SSC}$, the pair content (n_e/n_p) must decrease with decreasing distance, down to the value determined by the condition given by equation (6).

At distances given by equation (21), the shortest variability timescale, as limited by the transverse size of the

source, is

$$t_{\rm obs,min} \simeq \frac{a}{c\Gamma_j} \sim \frac{r}{c\Gamma_j^2} \sim 3 \times 10^6 r_{\rm SSC,19} \left(\frac{\Gamma_j}{10}\right)^{-2} \ {\rm s} \ . \quad (22)$$

The above limit comes independently from the minimum difference of optical paths of photons emitted from two opposite sides of a jet, $t_{\rm obs} \gtrsim a \sin\theta_{\rm obs}/c \simeq a/c\Gamma_j$, and from causality considerations, $t_{\rm obs} \simeq t'/\Gamma_j \geq a/c\Gamma_j$. With this limit, the SSC model cannot be applied to explain the γ-ray flares, which are often observed on timesscales shorter than ~ 1 week.

3.3. *Constraints on ERC Models*

3.3.1. *Poynting Flux*

In the case of ERC model we have

$$\frac{L'_C}{L'_S} \sim \frac{u'_D}{u'_B} \ , \quad (23)$$

but in contrast to the case of the SSC model, here in general $L_C/L_S \neq L'_C/L'_S$. This is because the ERC radiation is more collimated than the synchrotron radiation (see Dermer 1995). Noting, however, that practically the whole radiation is beamed quasi-uniformly within $\theta_j \sim 1/\Gamma_j$, the effect of the additional collimation in the ERC process is expected to be significant only for $\theta_{\rm obs} > 1/\Gamma_j$, and the relation $L_C/L_S \sim L'_C/L'_S \sim u'_D/u'_B$ can be applied for any observers located at $\theta_{\rm obs} \lesssim 1/\Gamma_j$. Combining this relation with the formula for u'_D (eq. [3] multiplied by Γ_j^2) we find that

$$u'_B \simeq \Gamma_j^2 \frac{\xi L_{\rm UV}}{4\pi r^2 c} \frac{L_S}{L_C} \ . \quad (24)$$

For steady flows, equation (24) gives

$$L_B \simeq c u'_B \pi r^2 \simeq 2.5 \times 10^{45} \frac{(\xi L_{\rm UV})_{45} L_{S,47}}{L_{C,48}} \ {\rm ergs \ s^{-1}} \ , \quad (25)$$

which is about 2 orders of magnitude greater than in the case of the SSC model.

3.3.2. *Electron Energies and Magnetic Fields*

In the case of the ERC model we have

$$\nu_C \simeq (\gamma'_b \Gamma_j)^2 \nu_{\rm UV} \ , \quad (26)$$

which gives

$$\gamma'_b \simeq \frac{1}{\Gamma_j} \left(\frac{\nu_C}{\nu_{\rm UV}}\right)^{1/2} = 0.6 \times 10^2 \left(\frac{\nu_{C,21}}{\nu_{\rm UV,15.5}}\right)^{1/2} \left(\frac{10}{\Gamma_j}\right) , \quad (27)$$

and from equations (17) and (27) we obtain magnetic field intensity

$$B' \simeq \frac{h\nu'_S/m_e c^2}{(\gamma'_b)^2} B_{\rm cr} \simeq 10^2 \frac{\nu_{S,13} \nu_{\rm uv,15.5}}{\nu_{C,21}} \frac{\Gamma_j}{10} \ {\rm gauss} \ . \quad (28)$$

Note that this magnetic field is roughly 4 orders of magnitude greater than that obtained for the SSC model (eq. [20]).

3.3.3. *Distance, Pair Content, and Variability Timescales*

Combination of equations (28) and equation (24) or equation (25) gives

$$r_{\rm ERC} \simeq 10^{16} \frac{\nu_{C,21}}{\nu_{S,13} \nu_{\rm UV,15.5}} \left[\frac{(\xi L_{\rm UV})_{45} L_{S,47}}{L_{C,48}}\right]^{1/2} {\rm cm} \ . \quad (29)$$

This is $\sim 10^2 r_g$ for the black hole of mass $10^9 M_\odot$, about 3 orders of magnitude smaller than $r_{\rm SSC}$, mainly due to much larger magnetic fields predicted in the ERC model than in SSC model (note that $r \propto L_B^{1/2}/B'$).

At such small distances, the condition $r_{\rm ERC} > r_{\rm min}$ (with $r_{\rm min}$ given by eq. [10]) can be satisfied only if

$$\frac{n_e}{n_p} < \frac{1}{2r_{g,14}} \frac{\nu_{C,21}}{\nu_{S,13} \nu_{\rm UV,15.5}} \frac{L_{\rm Edd}}{L_K} \frac{L_{S,47}^{1/2} L_{\rm SX,46}}{L_{C,48}^{1/2} [(\xi L_{\rm UV})_{45}]^{1/2}} \left(\frac{\Gamma_j}{10}\right)^{-3} , \quad (30)$$

where $r_{g,14} = r_g/10^{14}$ cm. This implies that jets in a viable ERC model must be free of pairs.

Minimum observed variability timescales due to the radiation emitted at distances as given by equation (27) are

$$t_{\rm obs,min} \sim 3 \times 10^3 r_{\rm ERC,16} \left(\frac{\Gamma_j}{10}\right)^{-2} {\rm s} \ , \quad (31)$$

sufficiently short to explain the rapid flaring activity observed in FSRQ.

4. THE MeV BREAK

4.1. *MeV Break in Compton Models*

One of the strongest constraints on the emission models of blazars is the spectral break ($\equiv$change of the power-law index) at the frequency where the luminosity peaks. Such breaks can have different origins: they can be related to the break in the electron injection function, as is assumed in homogeneous SSC models (Ghisellini et al. 1996; Mukherjee et al. 1996); they can result from incomplete cooling of relativistic electrons below a given energy, as is predicted by the homogeneous version of ERC model by SBR; they can reflect the electron spectrum shaped by the pair cascade process, as in the inhomogeneous ERC model suggested by Blandford & Levinson (1995); and, finally, they can correspond to the maximum injected electron energies at a distance where luminosity peaks are produced, provided such inhomogeneous models do not involve pair cascades.

The most severe constraints on nature of the spectral breaks come from the γ-ray observations. There, the spectral breaks, observed directly or deduced from extrapolation of the EGRET and X-ray spectra, have a remarkably "stable" location, usually in the 1–30 MeV range (see, e.g., von Montigny et al. 1995). Noting that in the homogeneous SSC models the photon energy at the Compton peak is $\propto(\gamma'_b)^4 B' \Gamma_j$, while in the homogeneous ERC models it is $\propto(\gamma'_b)^2 \Gamma_j^2$, this apparent stability of the location of the MeV breaks seems to require more fine-tuning (as applied to individual sources) of the parameters of the SSC models than of the ERC models.

Natural explanation of the location of the MeV spectral break is provided by an inhomogeneous version of the ERC model proposed by Blandford & Levinson (1995). In their model, the high-energy spectrum is produced by a Compton pair cascade, with the γ-ray portion above ~ 10 MeV resulting from a superposition of differential spectra produced over several decades of distance. These differential spectra have cutoffs due to γ-γ pair production on external X-rays, and, since the compactness of the external radiation drops with a distance, the energy of these cutoffs increases with distance. Hence, according to this model, the location of the break at MeV energies is determined by the position

of the high-energy cutoff of the spectrum produced by pair cascades at smallest distances. However, as was already pointed out by Ghisellini & Madau (1996), pair cascades produce X-ray spectra with the slopes $\alpha_X \geq 0.75$, which is larger than observed in most FSRQs (Worrall & Wilkes 1990; Kii et al. 1992; McNaron-Brown et al. 1995). Another difficulty with such a model is related to the constraint on the pair content; again, as discussed in § 2, this arises from the FSRQ spectra and, specifically, from the absence of soft X-ray excesses predicted via the bulk Compton process. This problem can conceivably be resolved by postulating moderate bulk Lorentz factor ($\lesssim 3$), but this would be in conflict with the unified scheme for FR II objects by predicting too many quasars with strong MeV peaks.

The prediction of the softer-than-observed X-ray spectra in the context of the inhomogeneous ERC models can be avoided if pair production is not involved. Then the X-ray slope and the MeV break correspond directly to the electron injection function at the base of the radiatively active region in a jet, whereas the slope of the γ-ray spectrum at >10 MeV depends on a distance distribution of both electron injection power and maximum electron energies. However, in this case, the position of the spectral break at MeV energies requires fine-tuning of the maximum energy of electrons (to the value given by eq. [27]) to correspond to the spectral region where the luminosity peaks are produced.

The homogeneous ERC model predicts that the break arises because of incomplete cooling of lower energy electrons, and its location can be made consistent with observations, provided that radiation is produced at distances 10^{17}–10^{18} cm from the central source (SBR). These particular distances can be related to the distance $\sim \Gamma_j^2 c\,\Delta t$ at which disturbances, separated by time Δt and propagating with a Lorentz factor different by $\Delta\Gamma \sim \Gamma_j$ collide and dissipate their energy (SBR). In such a scenario, Δt determines the timescale of γ-ray flares, which in several blazars has been observed to be ~ 1 day. This timescale corresponds roughly to the dynamical timescale of an accretion flow in the vicinity of a black hole of a mass of $10^9\,M_\odot$. The models then predict a change of the spectral slope around the break of $\Delta\alpha = \alpha_\gamma - \alpha_X = 0.5$. This is adequate to explain the observed breaks in most FSRQs; however, for some objects, this break is as large as $\Delta\alpha \sim 1$ (McNaron-Brown et al. 1995; Blom et al. 1995; Bloemen et al. 1995), and this cannot be explained as resulting from incomplete cooling effects. We discuss below possible modification of an ERC model, which can explain the extreme cases, i.e., the objects with the sharpest MeV peaks.

4.2. *The "Hot Electron" Scenario*

Let us assume that a roughly equal amount of energy necessary to stochastically accelerate relativistic electrons producing EGRET spectra is also used to heat *all* electrons. Such heating at subparsec distances is then balanced by energy losses due to radiation, and since radiative efficiency drops with increasing distance, at some point the electron "temperature" would reach the value corresponding to γ_b' given by equation (27). If the distance at which this occurs corresponds with the distance where the jet dissipates most of its energy, the Comptonization of external radiation by such mildly relativistic, "hot" electrons would lead to a formation of MeV bump. We show below that this is a viable scenario, but only if the plasma is pair-free. We also show that the region of the greatest energy dissipation, just as for the "cold" ERC model, is determined by the dynamical timescale of the central engine.

According to our assumptions

$$L_{\rm heat} = L_{\rm ERC,em} \simeq m_e c^2 \left| \frac{d\gamma_e}{dt} \right|_{\rm ERC} n_e\, \pi a^2\, \Delta r\ , \qquad (32)$$

where $\Delta r \simeq 2r - r$ is the region where the jet energy dissipation is largest, and, as shown by Sikora et al. (1996),

$$\left| \frac{d\gamma_e}{dt} \right|_{\rm ERC} \simeq \left| \frac{d\gamma_e'}{dt'} \right|_{\rm ERC} \simeq \frac{16}{9} \frac{c\sigma_{\rm T}}{m_e c^2} (\gamma_e' \Gamma_j)^2 u_D\ . \qquad (33)$$

Assuming that jet is steady, we have $L_{\rm ERC,em} \simeq L_C/2\Gamma_j^2$ (see Appendix A), and, using equation (8) for n_e, we find that the energy balance (eq. [32]) is satisfied if

$$(\gamma_e')^2 \simeq \frac{1}{4} \frac{n_p}{n_e} \frac{L_{\rm Edd}}{L_K} \frac{L_C}{\xi L_{\rm UV}} \frac{r}{r_g} \frac{1}{\Gamma_j^3}\ . \qquad (34)$$

Now, taking into account that the production of the MeV bump by upscattering of UV photons requires $\gamma_e \simeq \gamma_b' \simeq (\nu_C/\nu_{\rm UV})^{1/2}$, we find that the distance at which electrons reach such equilibrium energies is

$$r_C \simeq 10^4 r_g \frac{n_e}{n_p} \frac{L_K}{L_{\rm Edd}} \frac{(\xi L_{\rm UV})_{45}}{L_{\rm C,48}}\ , \qquad (35)$$

i.e., $\sim 10^{18} (M_{\rm BH}/10^9\ M_\odot)$ cm for powerful ($L_K \sim L_{\rm Edd}$) jets made from proton-electron ($n_e = n_i$) plasma.

We note that the same result also applies to the case of MeV radiation produced by moving "blobs," provided their sizes are $a \sim r/\Gamma_j$. In this case, $L_{\rm ERC,em} \sim L_C/\Gamma_j^4$. However, taking into account that the longitudinal size of the "blob," as measured in the black hole frame, is $a_\parallel \sim a/\Gamma_j \sim r/\Gamma_j^2$, we have now $\Delta r \sim r/\Gamma_j^2$, and both changes, one in the luminosity amplification, and the other in Δr, cancel each other in equation (32). Therefore, as long as the electron densities are the same in both cases, the distance estimate given by equation (35) is also valid for the "blob" models.

This "hot jet" scenario, suggested above to explain the MeV bumps, must be augmented by radiation processes responsible for GeV γ-ray and X-ray emission. The former can be produced by ultrarelativistic electrons accelerated to GeV energies by the first-order Fermi mechanism in collisionless shocks, while the latter (X-rays) can be produced by synchrotron-self Compton mechanism, as well as by hot plasmas at lower distances where the equilibrium electron energies are lower. The electron heating postulated in the above picture can be provided by reconnection of magnetic fields (Romanova & Lovelace 1992; Blackman 1996) or by acceleration of electrons by whistler waves (Dermer, Miller, & Li 1996; Levinson 1996b), and such electrons, preheated up to mildly relativistic energies, can be further efficiently accelerated in shocks.

5. DISCUSSION AND SUMMARY

Even the most precise imaging observations of blazars at any wavelength cannot resolve the innermost regions of their jets, and therefore we must use the spectral and variability data to study their structure, as well as the processes responsible for the acceleration and radiative output of the jets. Perhaps the most stringent constraints arise from the observations of those blazars that are associated with

quasars. These objects—flat spectrum radio quasars, or FSRQs—in addition to the nonthermal jet radiation that dominates spectra of BL Lac objects, also exhibit thermal signatures commonly observed in most AGN. These are broad emission lines that are visible even during high states of jet activity (Impey, Lawrence, & Tapia 1991), UV excesses that are observed during low states of jet activity (Smith et al. 1988; Brown et al. 1989a) or inferred from the decrease of the polarization level with frequency (Wills et al. 1992), and IR thermal radiation deduced from observations of spectral variability (Brown et al. 1989b). These features support the view that FSRQs are the radio-loud quasars observed along the jet. Since propagation of such a jet through dense radiation fields in quasars leads to Comptonization of this radiation and beaming of it along the jet, one can expect to see signatures of this process in spectra of FSRQs. These signatures are likely to impose additional constraints on physical parameters of jets and jet radiation models.

We first studied Comptonization of external radiation field by cold electrons in a jet. These electrons, streaming with Lorentz factor $\Gamma_j \sim 10$, scatter the external UV photons and produce a collimated beam of bulk Compton radiation, which is expected to arise in the soft X-ray regime. Its luminosity drops with the distance r as ξ/r, and therefore it is the highest close to the "base" of a jet, below which the jet is not yet fully developed (collimated, accelerated, and/or mass loaded). Comparing the results of our bulk Compton radiation calculations with the observed soft X-ray fluxes, we found that jets must be optically very thin (see eq. [6]), which excludes the importance of any such processes as pair annihilation, bremsstrahlung, and Coulomb interactions. Combining the limit for optical depth with the given kinetic energy flux in a jet, we derived lower limit for a distance of the jet base from the black hole. For the jets with the kinetic energy flux comparable to the Eddington luminosity, this distance is about $200(n_e/n_p)r_g$ (see eq. [10]). This seriously hampers all models predicting formation of pair-dominated jets closely to the black hole.

The detailed studies of Comptonization of external radiation by electrons with relativistic random energies in a jet are more ambiguous. This is because the distribution of *relativistic* plasma in a jet is related to the distribution of dissipative processes, which generally does not have to scale with the density of the *bulk* (cold) plasma in a jet. In addition, the ERC process leads to the production of a spectral component which largely overlaps with the SSC component, and only indirect arguments can determine whether the ERC component indeed dominates the observed spectrum. Comparing the energy densities of the synchrotron radiation field and the external diffuse radiation field, both as measured in the jet comoving frame, we concluded that the ERC process dominates if $\xi > 10^{-3}/(\Gamma_j/10)^4$ (see eq. [13]). This condition can be easily satisfied in quasars, where the values of ξ on the order of 0.01–0.1 can be provided by coronae/winds associated with the accretion disk and, at larger distances, by broad emission lines and dust radiation. For BL Lac objects, which do not show any distinctive signatures of thermal radiation and broad emission lines, the production of γ-rays can well be dominated by the SSC process.

Since both the SSC and the ERC processes are likely to operate in FSRQs at some level, we considered the broadband spectra of these objects to derive constraints on models based on both processes. We used luminosities of synchrotron and Compton components to calculate the Poynting flux in a jet (eqs. [16] and [25]) and location of the luminosity peaks to calculate the magnetic fields and energies of electrons producing the peaks (eqs. [19], [26], [27], and [28]). By combining the estimates of Poynting fluxes and magnetic fields, we obtained the distance r of the region in a jet where the most of radiation observed at the luminosity peaks is produced (eqs. [21] and [29]); and requiring that this distance is at $r \geq r_{\rm min}$, with $r_{\rm min}$ obtained from the constraint imposed on bulk Compton process by the observed X-ray luminosities, we derived the upper limits for the electron-positron pair content in the jet plasma. The two most important constraints from these analyses are that in the strongly γ-ray–dominated FSRQs, the Poynting flux in the SSC jet models must be ~ 3 orders of magnitude lower than the kinetic energy flux determined from radio-lobe studies (Rawlings & Saunders 1991), and that in the ERC models, the peak luminosities must be produced very closely to the black hole. We stress, however, that all results obtained using the luminosities and energies of the two spectral peaks are valid only if these peaks are produced *both* in the same spatial region and by electrons with the same energy.

Finally, we discussed the difficulties that different radiation models have in explaining the "stable" location of the peak at MeV energies. Most natural explanation of this peak is provided by the inhomogeneous version of the ERC model proposed by Blandford & Levinson (1995), where the location of the peak at a few MeV is explained by the γ-γ absorption of high-energy radiation produced most closely to the black hole. However, as was pointed out by Ghisellini & Madau (1996), such a model predicts a stronger than observed relative X-ray luminosity. An alternative explanation of the MeV break/peak is provided by the homogeneous version of ERC model by SBR. According to this model, the break results from incomplete cooling of electrons below a given energy. This energy is determined by equating the ERC energy losses timescale to the jet dynamical timescale and corresponds to the peak at MeV energies if the radiation is produced at distances $\sim 10^{17}$–10^{18} cm. These are distances required to produce the γ-ray flares with the observed timescales of ~ 1 day. Such distances, implied by homogeneous ERC models as sites for the γ-ray production, are much larger than these obtained from the two-peak luminosity analyses (see eq. [29]). This discrepancy can be resolved by postulating different regions of production of two peaks or by postulating that magnetic field is not homogeneous and that the more energetic electrons cool in stronger magnetic fields (on average) than less energetic electrons. The change of the spectral slope due to the incomplete cooling is $\Delta\alpha \simeq 0.5$, and, with adding some contribution from lower distance jet parts, one in principle could explain the spectra of all MeV radiation dominated blazars, as long as $\Delta\alpha \lesssim 0.5$. However, there are known cases with $\Delta\alpha \sim 1$ (McNaron-Brown et al. 1995; Blom et al. 1995; Bloemen et al. 1995), which cannot be explained by any previous models.

To explain such spectra, we proposed the "hot electron" version of the ERC scenario, where a similar fraction of energy dissipated in the jet is channeled to heat electrons as that required to accelerate some of them further in shocks. We found that electron "temperatures" of ~ 100 MeV, required to produce the MeV bump, are available at dis-

tances 10^{17}–10^{18} cm, provided the plasma is not dominated by pairs (i.e., $n_e \sim n_p$). In this scenario, the γ-ray spectra at higher energies (>100 MeV) are produced by electrons further accelerated by shocks up to GeV energies. Since all electrons are assumed to be preheated up to 100 MeV energies before being accelerated to higher energies, the ERC process, operating at a distance where the MeV peak is produced, does not contribute to the X-ray spectra. The X-rays can be produced by a synchrotron self-Compton mechanism and/or by hot plasmas at lower distances, where equilibrium temperatures are lower. Such efficient electron heating is also desired for two other reasons: it provides the precondition for effective acceleration of electrons in shocks (Romanova & Lovelace 1992; Blackman 1996; Levinson 1996b), and, via dramatic reduction of the density of cold electrons, it solves the problem of Faraday depolarization in proton-electron jets (Wardle 1977; Jones & O'Dell 1977).

In all SSC and ERC models discussed in this paper, electrons are assumed to be accelerated directly or produced by photon-photon interactions. Alternatively or additionally, relativistic electrons can be injected by relativistic protons following nuclear interactions and/or photo-meson production process. Since the column densities in the jet plasma are too low to provide a target for nuclear interactions, an external target has been postulated (Bednarek 1993). Such a target can be provided by the walls of the funnels formed around the black hole by a geometrically thick disk. There are at least two shortcomings of such a model: first, the extremely low magnetic fields in the target are required to avoid isotropization of relativistic protons before nuclear collisions, and second, such a compact region is expected to be opaque for GeV photons. For the photo-meson production, injection of relativistic electrons is limited by requiring extremely relativistic protons. Only for protons with energies above $\sim 10^9$ GeV, the blazar radiation fields become opaque for photo-meson production process (Mannheim 1993). Following photo-meson production triggered by such protons, the synchrotron pair cascade develops. In this model, the break between X-rays and γ-rays is postulated to correspond with the break in the pair injection function. The model predicts $\alpha_\gamma \leq 1$, and therefore it cannot explain production of γ-rays in blazars with steep γ-ray spectra.

We would like to thank the referee, Gabriele Ghisellini, for his constructive comments, which helped us to significantly improve this paper. M. S. would like to acknowledge support from ITP and Stockholm Observatory where part of this work has been accomplished. G. M. is grateful for the hospitality of JILA, where many initial discussions leading to this paper took place. The research was supported by NASA grants NAG 5-2439 (G. Madejski, PI) and NAG 5-2026 (M. Begelman, PI), NSF grant PHY 94-07194, the Polish KBN grants 2P03D01209 and 2P03D01010, and by grants from the Swedish Natural Science Research Council and Stockholm University.

APPENDIX A

LUMINOSITY AMPLIFICATION IN STEADY-STATE JET MODELS

The observed luminosity for a zero redshift objects is defined as

$$L_{\rm obs} = 4\pi d_L^2 F_{\rm obs} , \tag{A1}$$

where d_L is the luminosity distance to the object,

$$F_{\rm obs} = \int I \, d\Omega , \tag{A2}$$

is the observed flux, and

$$I = \int j \, ds , \tag{A3}$$

where j is the volume emissivity in the direction to the observer, ds is a distance measured along the ray within the source, and the source is assumed to be optically thin. Noting that $d\Omega = dA/d_L^2$, where A is an element of area in the pattern frame that for a steady-state jet has zero velocity (see, e.g., Lind & Blandford 1985), we obtain that

$$F_{\rm obs} = \frac{1}{d_L^2} \int j \, dV , \tag{A4}$$

where $dV = dA\, ds$. Now, using Lorentz transformation formulae $j = \mathscr{D}^3 j'$ and $V = V'/\Gamma_j$, we obtain

$$L_{\rm obs} = 4\pi \frac{\mathscr{D}^3}{\Gamma_j} \int j' \, dV' , \tag{A5}$$

where $\mathscr{D} = [\Gamma_j(1 - \beta \cos \theta_{\rm obs})]^{-1}$. (Note that relation $\int j \, dV = (\mathscr{D}^3/\Gamma_j) \int j' \, dV'$ corresponds directly to the relation given by Rybicki & Lightman 1979 between the power emitted per solid angle as measured in the comoving frame and the power emitted per solid angle as measured in the external frame.) If the radiation in the jet frame is isotropic, then $4\pi \int j' dV'$ is equal to the total emitted luminosity L', and

$$L_{\rm obs} = \frac{\mathscr{D}^3}{\Gamma_j} L' . \tag{A6}$$

Taking into account that for an axisymmetric emissivity j'

$$L_{\rm em} = \oint \frac{\partial L_{\rm em}}{\partial \Omega}\, d\Omega = \oint \frac{\mathscr{D}^3}{\Gamma_j} \frac{\partial L'}{\partial \Omega'}\, d\Omega' = L' \,, \tag{A7}$$

where $\partial L_{\rm em}/\partial\Omega \equiv \int j\, dV$ and $\partial L'/\partial\Omega' \equiv \int j'\, dV'$, we obtain

$$L_{\rm obs} = \frac{\mathscr{D}^3}{\Gamma_j} L_{\rm em} \,. \tag{A8}$$

Equation (A8) is, however, derived for $\theta_j = 0$ and provides a good approximation of luminosity amplification only for $\theta_j < 1/\Gamma_j$. For jets with $\theta_j \gtrsim 1/\Gamma_j$, the dependence of the observed luminosity on $\theta_{\rm obs}$ is flat and for $\theta_j \gg 1/\Gamma_j$ is well approximated by

$$L_{\rm obs} \simeq \frac{4\pi}{\Omega_j} L_{\rm em} \,, \tag{A9}$$

where $\Omega_j \simeq \pi\theta_j^2$. (Note that for a spherical outflow, $L_{\rm obs} = L_{\rm em}$, as one should expect for steady-state sources.)

In our paper we assumed that $\theta_j \sim 1/\Gamma_j$ and $\theta_{\rm obs} \sim 1/\Gamma_j$, and for such a case, none of the two analytical approximations works well. Equation (A8) for $\theta_{\rm obs} = 1/\Gamma_j$ gives $L_{\rm obs} = \Gamma_j^2 L_{\rm em}$, while equation (A9) for $\theta_{\rm obs} = 1/\Gamma_j$ gives $L_{\rm obs} = 4\Gamma_j^2 L_{\rm em}$. We found numerically that the correct value is almost exactly intermediate, i.e.,

$$L_{\rm obs} \simeq 2\Gamma_j^2 L_{\rm em} \,. \tag{A10}$$

APPENDIX B

STEADY-STATE SOURCES VERSUS MOVING BLOBS

The commonly used term "blob" in reference to blazars has no unique meaning. In the extreme case, a "blob" is understood as representing isolated portion of plasma with associated magnetic fields. Presumably, a more realistic meaning of a "blob" is that it represents some inhomogeneity propagating along a jet (e.g., a shock) where the dissipation of bulk kinetic energy and/or magnetic fields leads to an acceleration of relativistic particles. In this case, the contrast between densities of the bulk matter (i.e., the portion of matter that dominates kinetic energy flux of a jet) and the magnetic field intensities *inside* and *outside* of the blob does not have to be very large, and then one can use "steady-state" scaling to determine these parameters in blobs as a function of a distance.

Another issue concerning the "blobs" and steady state sources regards the proper form of the luminosity amplification formula. Specifically, what are the circumstances when one should use $L_{\rm obs} = \mathscr{D}^4 L'_{\rm blob}$, and when equation (A8) should be applied? To answer this question in an illustrative way, below we use a simple model, where the jet is represented by a sequence of blobs/inhomogeneities propagating along a given direction.

Let us assume that (1) the blobs are injected into the "active zone" every $\Delta t_{\rm inj}$; (2) all blobs are moving with the same Lorentz factor; (3) blobs radiate isotropically in their rest frame, each at the same rate, $L'_{\rm em,1}$; (4) each blob stops to radiate after passing a given distance range $\Delta r = r$.

Since in the external frame (in which the black hole and noncosmological distant observers are at rest) blobs are moving at a speed βc, the number of blobs enclosed within a distance range $\Delta r = r$ is

$$\mathscr{N} = \frac{\Delta t_{\rm em}}{\Delta t_{\rm inj}} \,, \tag{B1}$$

where $\Delta t_{\rm em} = r/\beta c$. Since the signal from each blob is observed during time (Rybicki & Lightman 1979)

$$\Delta t_{\rm obs}(\theta_{\rm obs}) = (1 - \beta \cos\theta_{\rm obs})\Delta t_{\rm em} \,, \tag{B2}$$

the number of blobs contributing at any moment to the observed radiation (observed separately on the sky, if we have sufficiently good angular resolution) is

$$\mathscr{N}_{\rm obs} = \frac{\Delta t_{\rm obs}}{\Delta t_{\rm inj}} = \frac{(1 - \beta \cos\theta_{\rm obs})\Delta t_{\rm em}}{\Delta t_{\rm inj}} = (1 - \beta \cos\theta_{\rm obs})\mathscr{N} \,. \tag{B3}$$

Then, noting that the luminosity observed from each blob is

$$L_{\rm obs,1}(\theta_{\rm obs}) = \mathscr{D}^4 L'_{\rm em,1} \,, \tag{B4}$$

we obtain that total observed luminosity is

$$L_{\rm obs}(\theta_{\rm obs}) = \mathscr{N}_{\rm obs}(\theta_{\rm obs}) L_{\rm obs,1}(\theta_{\rm obs}) = \mathscr{N}(1 - \beta \cos\theta_{\rm obs})\mathscr{D}^4 L'_{\rm em,1} = \frac{\mathscr{D}^3}{\Gamma_j} L'_{\rm em} \,, \tag{B5}$$

where $L'_{\rm em} = \mathscr{N} L'_{\rm em,1}$. Since blobs are assumed to radiate isotropically in their respective rest frames, we have $L_{\rm em} = L'_{\rm em}$ and from equation (B5) we obtain equation (A8).

It is important to emphasize that as long as we consider the luminosity that is emitted only by these blobs, which at a given moment contribute to the observed flux, then, just as in the case of luminosity amplification for a single blob, we have

$$L_{\rm obs} = \mathcal{N}_{\rm obs} L'_{\rm em,1} \mathcal{D}^4 = L'_{\rm em}(\mathcal{N}_{\rm obs})\mathcal{D}^4 = L_{\rm em}(\mathcal{N}_{\rm obs})\mathcal{D}^4 \ . \tag{B6}$$

Let us assume now that $\Delta t_{\rm inj} = \Delta t_{\rm obs}(\theta_{\rm obs} = 1/\Gamma_j)$, i.e., that at any moment only one blob is seen by the observer located at $\theta_{\rm obs} = 1/\Gamma_j$ (see eq. [B3]) and that blobs have longitudinal sizes $a_{\parallel} = c\beta\Delta t_{\rm inj}$, i.e., that they form continuous pattern, which within a distance range $\Delta r = r$ produces radiation in a steady-state manner. Then, it *does not matter* that there is only one blob or continuous steady pattern: the observer sees the same luminosity in both cases (see eq. [B6] for $\mathcal{N}_{\rm obs} = 1$), and the radiation energy density given by equation (11) for a single blob applies for steady sources as well.

REFERENCES

Bednarek, W. 1993, ApJ, 402, L29
Begelman, M. C., & Sikora, M. 1987, ApJ, 322, 650
Blackman, E. G. 1996, ApJ, 456, L87
Blandford, R. D., & Königl, A. 1979, ApJ, 232, 34
Blandford, R. D., & Levinson, A. 1995, ApJ, 441, 79
Blandford, R. D., & Payne D. G. 1982, MNRAS, 199, 883
Blandford, R. D., & Rees, M. J. 1978, in Pittsburgh Conference on BL Lac Objects, ed. A. N. Wolfe (Pittsburgh: Pittsburgh Univ. Press), 328
Blandford, R. D., & Znajek, R. L. 1977, MNRAS, 179, 433
Bloemen, H., et al. 1995, A&A, 293, L1
Blom, J. J., et al. 1995, A&A, 298, L33
Brown, L. M. J., et al. 1989a, ApJ, 340, 129
Brown, L. M. J., Robson, E. I., Gear, W. K., & Smith, M. G. 1989b, ApJ, 340, 150
Coppi, P., & Blandford, R. 1990, MNRAS, 245, 453
Dermer, C. D. 1995, ApJ, 446, L63
Dermer, C. D., Miller, J. A., & Li, H. 1996, ApJ, 456, 106
Dermer, C. D., & Schlickeiser, R. 1993, ApJ, 416, 458
Dermer, C. D., Schlickeiser, R., & Mastichiadis, A. 1992, A&A, 256, L27
Ghisellini, G., & Madau, P. 1996, MNRAS, 280, 67
Ghisellini, G., & Maraschi, L. 1989, ApJ, 340, 181
Ghisellini, G., Maraschi, L., & Dondi, L. 1996, A&AS, 120, C503
Impey, C. D., Lawrence, C. R., & Tapia, S. 1991, ApJ, 375, 46
Jones, T. W., & O'Dell, S. L. 1977, A&A, 61, 29
Kii, T., et al. 1992, in Frontiers of X-Ray Astronomy, ed. Y. Tanaka & K. Koyama (Tokyo: Universal Academy Press), 577
Königl, A. 1981, ApJ, 243, 700
Levinson, A. 1996a, ApJ, 467, 546
Levinson, A. 1996b, MNRAS, 278, 1018
Levinson, A., & Blandford, R. D. 1995, ApJ, 449, 86
Lind, K. R., & Blandford, R. D. 1985, ApJ, 295, 358
Mannheim, K. 1993, A&A, 269, 67
Maraschi, L., & Rovetti, F. 1994, ApJ, 436, 79
Marscher, A., & Gear, W. 1985, ApJ, 198, 114
McNaron-Brown, K., et al. 1995, ApJ, 451, 575
Mukherjee, R., et al. 1996, ApJ, 470, 831
Padovani, P., & Urry, C. M. 1992, ApJ, 387, 449
Rawlings, S., & Saunders, R. 1991, Nature, 349, 138
Rees, M. 1967, MNRAS, 137, 429
Romanova, M. M., & Lovelace, R. V. E. 1992, A&A, 262, 26
Rybicki, G. B., & Lightman, A. P. 1979, Radiative Processes in Astrophysics (New York: Wiley)
Sikora, M. 1994, ApJS, 90, 923
Sikora, M., Begelman, M. C., & Rees, M. J. 1994, ApJ, 421, 153 (SBR)
Sikora, M., Sol, H., Begelman, M. C., & Madejski, G. M. 1996, MNRAS, 280, 781
Smith, P. S., Elston, R., Berriman, G., & Allen, R. G. 1988, ApJ, 326, L39
Svensson, R. 1987, MNRAS, 227, 403
Vermeulen, R. C., & Cohen, M. H. 1994, ApJ, 430, 467
von Montigny, C., et al. 1995, ApJ, 440, 525
Wardle, J. F. C. 1977, Nature, 269, 563
Wills, B. J., Wills, D., Breger, M., Barvainis, R. 1992, ApJ, 398, 454
Worrall, D. M., & Wilkes, B. J. 1990, ApJ, 360, 396